LIMNOLOGY
and
OCEANOGRAPHY

ASLO

Limnol. Oceanogr. 00, 2017, 00–00

doi: 10.1002/lno.10680

A self-cleaning biological filter: How appendicularians mechanically control particle adhesion and removal

Keats R. Conley [1]*, **Brad J. Gemmell,** [2] **Jean-Marie Bouquet,** [3] **Eric M. Thompson,** [3] **Kelly R. Sutherland** [1]

[1]Department of Biology, University of Oregon, Eugene, Oregon
[2]Department of Integrative Biology, University of South Florida, Tampa, Florida
[3]Sars Centre and Department of Biology, University of Bergen, Bergen, Norway

Abstract

Appendicularians are ubiquitous marine grazers that use tangential filtration to collect micron and submicron prey. The food-concentrating filter (FCF) is the primary determinant of appendicularian prey selectivity, but the precise means by which it concentrates and conveys particles to the pharyngeal filter remain poorly understood. We used high-speed videography to examine the mechanics of the FCF of *Oikopleura dioica* with high resolution to better understand how filter structure, hydrodynamics, and animal behavior affect feeding selectivity. We observed that filtration occurs through the process of serial adhesion and detachment of particles, and in this respect, differs from an industrial tangential filtration system. We demonstrate how filter elasticity and the hydrodynamics of pulsatile flow caused by the kinematics of the animal's tail contribute to the filter's self-cleaning abilities. We present experimental observations showing that smaller particles (3 μm) adhere significantly more to the filter than larger ones (10 μm), but that, overall adhesion is quite low for an array of particle sizes (3–20 μm). This study provides a mechanistic basis for predicting the effects of appendicularian grazing on particle size spectra in the upper ocean.

Planktonic grazers influence particle size structure, plankton diversity, and energy transfer in aquatic food webs (Sommer and Stibor 2002). Their influence depends upon the structure of the feeding apparatus and the hydrodynamic aspects of particle capture. Numerous grazers, such as pteropods, tunicates, lancelets, chaetopeterid polychaetes, and certain gastropods, rely on a mucous filter to capture suspended prey—typically ingesting the entire mesh along with retained food particles (Riisgård and Larsen 2001). Suspended particles may either travel perpendicular to the filter (sieving) or parallel to it (tangential filtration). If suspension feeding occurs solely via sieving, the filter only retains particles larger than the mesh pores; whereas, in tangential filtration, fewer particles directly contact the filter and they become concentrated as water is extruded through the filter (Brainerd 2001). The mechanisms by which a biological filter captures particles have broad implications for feeding efficiency and particle size-selection (Rubenstein and Koehl 1977).

Appendicularians (Phylum: Chordata, Subphylum: Tunicata) are a class of globally abundant, planktonic marine grazers that can filter-feed on particles several orders of magnitude smaller than themselves, down to picoplankton (0.2–2 μm) (Acuña et al. 1996; Gorsky and Fenaux 1998). Appendicularians have both an internal filter (the pharyngeal filter) and an extracellular mucous filtration apparatus called the house (Fig. 1). The appendicularian house is one of the most intricate structures made by an animal (Alldredge 1977). It is a spherical extracellular secretion that the animal lives inside and uses to concentrate prey particles from seawater. Appendicularian filtration shares the fundamental particle interception mechanisms employed by numerous filter-feeders, including sieving, direct interception, and diffusional deposition (Acuña et al. 1996).

The Oikopleurid house (Class: Appendicularia, Family: Oikopleuridae) has two distinct mucous filters: inlet filters (IF) and the food-concentrating filter (FCF) (Fig. 1). Particles that adhere to the FCF need to detach in order to be subsequently conveyed through the FCF to the internal pharyngeal filter for ingestion (Deibel 1988; Morris and Deibel 1993). Therefore, the degree of adhesion by different particle types governs both retention in the house and ingestion by the animal. The composition of particles retained by the house has important implications for biogeochemical cycling because discarded appendicularian houses are a major source of particulate organic carbon in the ocean, possibly even exceeding phytoplankton carbon (Alldredge 1976; Katija

*Correspondence: keatsconley@gmail.com

Additional Supporting Information may be found in the online version of this article.

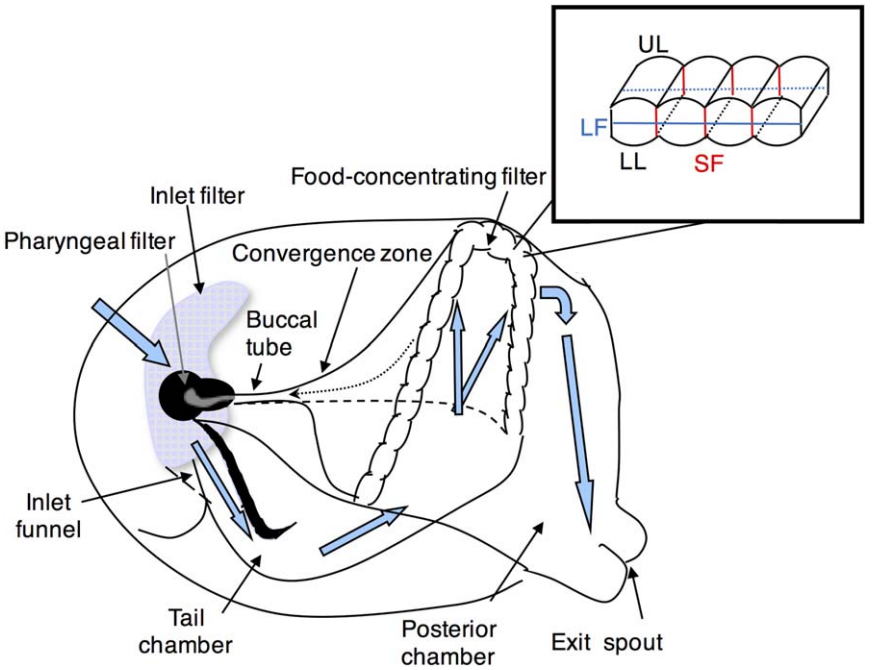

Fig. 1. Schematic representation of the Oikopleurid house structure and water circulation (thick arrows) (modified from Thompson et al. 2001). Inset shows magnified view of the FCF slots and the intermediate layer, composed of the lateral fibers (LF) and suspensory fibers (SF). LL, lower layer; UL, upper layer. [Color figure can be viewed at wileyonlinelibrary.com]

et al. 2017). The particles that are conveyed to the pharyngeal filter for ingestion by the animal are either incorporated into animal biomass for subsequent transfer within the pelagic food web, or into fecal pellets that contribute to the flux of carbon to depth.

During feeding, sinusoidal beats of the animal's tail bring water into the house and control water flow through the house. There are also periodic tail arrests, where the tail abruptly straightens. The house is elastic, and the tail beat and arrest cycles alternately expand and contract the house (Selander and Tiselius 2003). The FCF, the focus of the present study, has a three-layered structure similar to that of a parafoil parachute (Fig. 1) and performs tangential filtration to concentrate particles (Morris and Deibel 1993). An upper (mesh dimensions: 0.98 $\times$ 0.15 μm, Flood and Deibel 1998) and lower (0.24 $\times$ 0.07 μm, Flood 1978; Morris and Deibel 1993) layer are held together by an intermediate screen that is connected to the filter ridges of the FCF by suspensory filaments with pores that are $\sim$ 30 μm wide (Flood 1991) (Fig. 1). Two ciliated funnels called spiracles generate a current to convey particles from the FCF through the buccal tube and into the mouth (Burighel et al. 2001; Lombard et al. 2011) (Fig. 1).

There is debate about how the FCF works, including the mechanisms controlling particle adhesion and detachment. The prevailing assumption has been that the fine lower layer of the FCF concentrates particles (Flood 1978), while the intermediate screen simply attaches the two layers (Deibel 1986). Since the pores of the intermediate screen are up to twice as wide as those of the IF, a possible straining function has been proposed (Alldredge 1977) and disputed (Flood 1991). Previously, pulsatile flow was suggested to play a role in the particle detachment process of the cold-water appendicularian *Oikopleura vanhoeffeni*, but this mechanism was not investigated in detail (Deibel 1988; Morris and Deibel 1993). Acquiring a better understanding of the mechanisms of filtration by the FCF is important because of the filter's remarkable capacity to concentrate particles up to 1000$\times$ that of ambient seawater (Morris and Deibel 1993). Furthermore, understanding the mechanisms of biological self-cleaning systems has practical applications for biomimetics (Liu and Jiang 2012).

In this study, our goal was to better understand how filtration apparatus structure, hydrodynamics, and animal behavior contribute to particle selection. Specifically, we tested three hypotheses: (1) that pulsed flow is the mechanism for particle detachment; (2) that no size-selection by the house occurs through particle interactions with the FCF; and (3) that the intermediate layer of the FCF plays a purely structural role.

Methods

Hydrodynamics of the appendicularian house and observations of feeding behavior

All visualizations were conducted at the Sars Centre for Marine Molecular Biology, Bergen, Norway, using cultured

Oikopleura dioica (Bouquet et al. 2009). We used high-resolution, high-speed microvideography to visualize the hydrodynamics of filtration within the house. The setup for visualizations followed that previously described (Gemmell et al. 2014). Briefly, an individual appendicularian (day 5 or 6) was added to a 50 mL glass cuvette. Flow was traced using live, unicellular microalgae *Rhinomonas reticulata* for observations of the whole house at low magnifications (4X) or *Isochrysis galbana* at high magnifications of particular areas (40X). Images were recorded using an Edgertronic high-speed camera (1280 × 1024 pixel resolution, 500 frames s^{-1}) with brightfield illumination from a fiber optic light source. The filming vessel was positioned on a manually adjustable stage between the light source and the camera. A long working-distance microscope objective (4X or 40X) was mounted to an adjustable-height optics clamp positioned between the filming vessel and the camera. For all videography, the period of animal containment never exceeded a few minutes.

Videos were converted to an image stack in QuickTime Pro. ImageJ software was used for subsequent velocity measurements. The speed of particles in the FCF was assessed by particle-tracking velocimetry, performed either manually, by tracking individual particles between frames using the plugin MTrackJ (Meijering et al. 2012), or automatically using the ParticleTracker plugin for videos with high particle densities. The instantaneous velocity of the filter fibers was measured as the change in arc length between the extended and relaxed fiber divided by the change in time. All results are reported as the mean ± 95% confidence interval from day 5 animals unless stated otherwise. *N* is used throughout to refer to the number of individual animals and *n* for number of observations. In all cases, *N* was used to calculate the confidence interval.

Particle adhesion to the FCF

To experimentally determine how particle size affects adhesion to the appendicularian FCF, we used latex microspheres that allowed us to maintain constant surface properties while varying only particle size. The animals were fed a mixture of different sized (3 μm, 6 μm, 10 μm, and 20 μm diameter) fluorescent polystyrene microspheres (Polysciences) (10^{-1}–10^{-2} beads mm^{-2} of FCF). To visualize bead interactions with the FCF, we used a Sony 4K FDR-AX100 HD camcorder (1280 × 720 pixel resolution, 120 frames s^{-1}) mounted to a Nikon Eclipse E400 microscope with a 10X objective using a Martin Microscope M99 Camcorder Adapter. Immature day 5 ($N = 5$) or day 6 ($N = 2$) animals were first placed in 0.2 μm filtered seawater (FSW) to inflate a new, clean house. Animals were then filmed individually in a glass embryo dish with a suspension of the microspheres.

Videos were converted to image stacks and analyzed using ImageJ as described above. Percentage particle adhesion was calculated by counting the number of microspheres adhering to the FCF immediately prior to a single tail arrest and then tracking the number of particles that detached or remained adhered after the FCF reinflated upon recommencement of tail beating. Only new adhesion events from incoming particles were analyzed (i.e., beads that were already stuck to the filter prior to commencement of videography were excluded from the analysis).

Statistical analysis

Analysis of size-dependent adhesion was conducted using R Studio (version 1.0.143 © 2009–2016) using particle size (3 μm, 6 μm, or 10 μm) as a predictor variable of percent adhesion to the FCF. Twenty-micron particles were excluded from statistical analysis because of the comparably low sample size for adhesion measurements ($n = 11$, $N = 3$). The distribution of percent adhesion did not adhere to the analysis of variance (ANOVA) assumption of normality (evaluated using a normal probability plot), and arcsin-transformed data still differed significantly from a normal distribution (Shapiro-Wilk normality test, $W = 0.749$, $p < 0.001$). Size-dependent adhesion was therefore tested using a nonparametric Kruskal-Wallis one-way ANOVA on ranks, followed by a Nemenyi test for pairwise multiple comparisons.

Morphology and function of the intermediate screen

The setup for visualizing the filtration apparatus structure was the same as that used for visualizing the hydrodynamics, except that animals were placed in a dilute milk (Tinemelk® low-fat milk, 1.2% fat) bath (~ 1 : 10,000 milk : seawater) to filter for ~ 1 h and then rinsed in clean seawater prior to videography. Deposition of milk fat particles facilitated visualizations of the filter fibers of the FCF intermediate screen. ImageJ was used for subsequent morphometric measurements.

Thin-section transmission electron microscopy of the spiracles

Specimens of *O. dioica* were fixed with 2.5% glutaraldehyde in 0.1M sodium cacodylate buffer using a procedure described by Brena et al. (2003). Samples were suspended in 3% low melting point agarose blocks to support the animals and dehydrated in a graded series of acetone, 30%, 50%, 75%, 95%, and three changes of 100%, each change for 15 min. Samples were infiltrated in LX 112 embedding resin mix 2 h and embedded in flat silicone rubber embedding molds. The embedding resin was polymerized at 70°C overnight. Samples were sectioned on a Leica Ultracut E ultramicrotome (Leica Microsystems, Buffalo Grove, Illinois). Sections were stained with 8% aqueous uranyl acetate and Reynold's lead citrate stains. Eighty nanometer sections were observed and photographed with an FEI Morgagni transmission electron microscope (FEI Company, Hillsboro OR.) at 60 kV using an AMT ActiveVu camera (Advanced Microscopy Techniques Corporation, Woburn, Massachusetts).

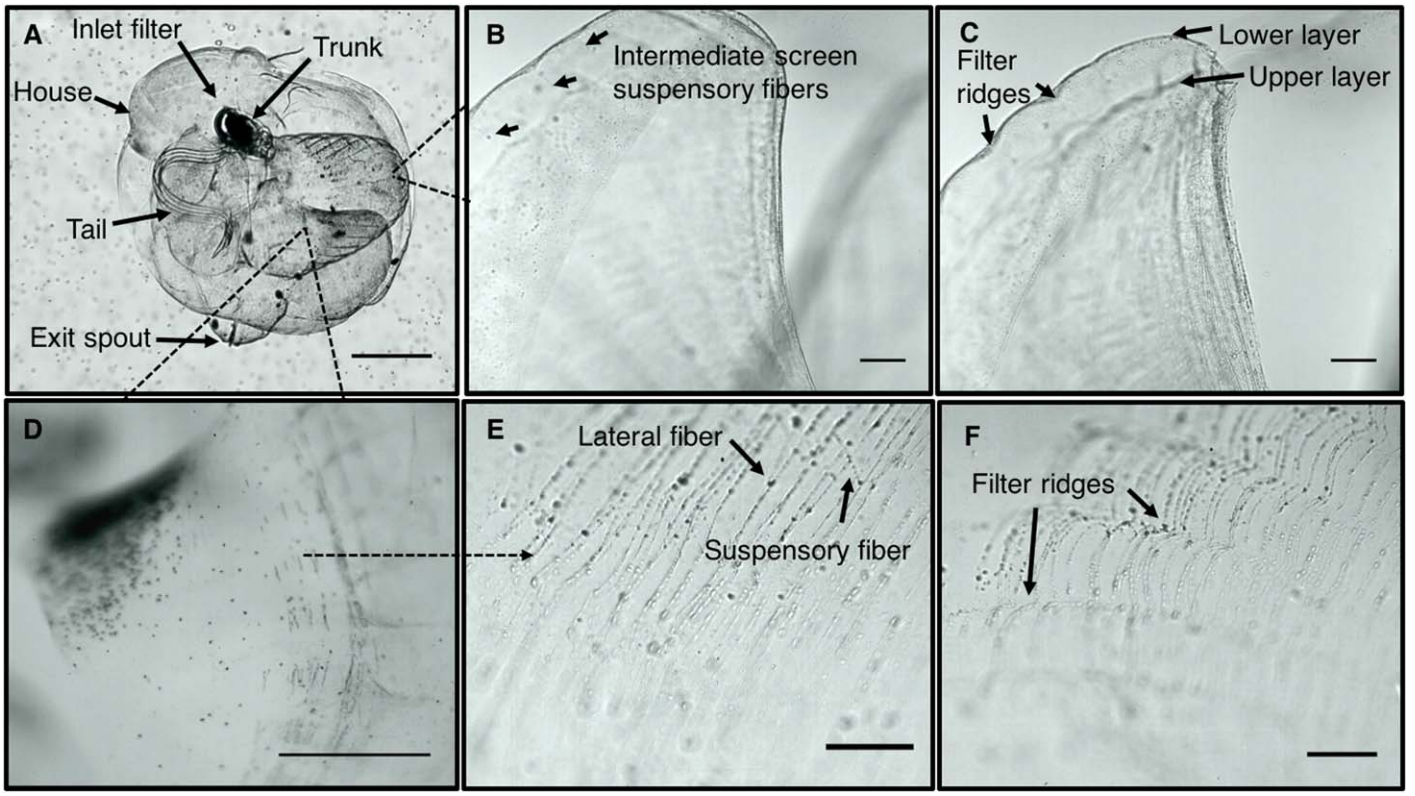

Fig. 2. Brightfield images extracted from microvideography of free-swimming *O. dioica* showing the effect of the tail beat and arrest cycle on the structure of the FCF. (**A**) *O. dioica* with *Rhinomonas* as tracer particles (4X objective). (**B**) Inflated wing of FCF during tail beat (40X objective). (**C**) Deflated wing of FCF during tail arrest. (**D**) Magnified view of the FCF showing fibers of intermediate screen (11.5X objective). (**E**) The extended fibers of the intermediate screen during tail beating (40X objective). (**F**) The compressed fibers of the intermediate screen during period of tail arrest (40X objective). Scale bars: (**A**, **D**): 0.5 mm; (**B**, **E**, **F**): 0.1 mm. [Color figure can be viewed at wileyonlinelibrary.com]

Results

Hydrodynamics of the appendicularian house

Appendicularians forced water into the house through the sinusoidal beating of the tail, which inflated the house like a balloon. The tail beat cyclically, alternating between continual beating and periodic tail arrests. The tail arrest partially deflated the house, whereby water exited out of the two IF and cleared accumulated particles from the inlet and FCFs as previously described (Deibel 1988; Flood 1991; Selander and Tiselius 2003). Alternation between tail beating and tail arrest not only deflated and reinflated the FCF (Fig. 2B,C), it also changed the shape of the individual mesh fibers of the intermediate layer (Fig. 2E,F; Supporting Information Video 1). The mesh fibers exhibited an elastic, accordion-like conformational change: when the house partially deflated during a tail arrest due to a presumed decrease in fluid pressure, the fibers bent and shortened. We were not able to resolve the individual fibers of the lower or upper layers of the FCF, but the elasticity of the intermediate fibers was mirrored by the entire FCF. When the house reinflated as the tail resumed beating, the bent fibers recoiled, which, in combination with the pulsatile flow induced by the tail, caused a pulse of previously-adhered particles to detach and travel down the filter toward the buccal tube (Fig. 3A,B; Supporting Information Video 2).

Particles that entered the FCF first adhered in an "adhesion zone" on the outer margin of the FCF, characterized by both low flow from the tail and low flow from the spiracles (Fig. 3C). An average of 90% ± 25% of *R. reticulata* that entered the FCF first adhered to the FCF prior to being conveyed to the pharyngeal filter ($n = 30$, $N = 3$). Particles also detached most frequently from the outer part of the FCF, opposite the trunk (Fig. 3A,B; Supporting Information Video 2). After detachment, particles were laterally conveyed toward the buccal tube at 1.35 ± 0.94 mm s^{-1} ($n = 3366$, $N = 8$). The percentage change in length of the fibers between their maximally contracted and extended state was 10% ± 16% ($n = 10$; $N = 3$). The average velocity of the fibers was 0.19 ± 0.57 mm s^{-1} ($n = 21$, $N = 3$), which gives a Reynolds number of 10^{-4} for individual filter fibers, calculated using diameter of the lateral fibers of the intermediate screen (~ 2 μm) as the characteristic length scale. The maximum measured instantaneous velocity of the fibers was 0.97 mm s^{-1}. The phases of particle adhesion and detachment to the

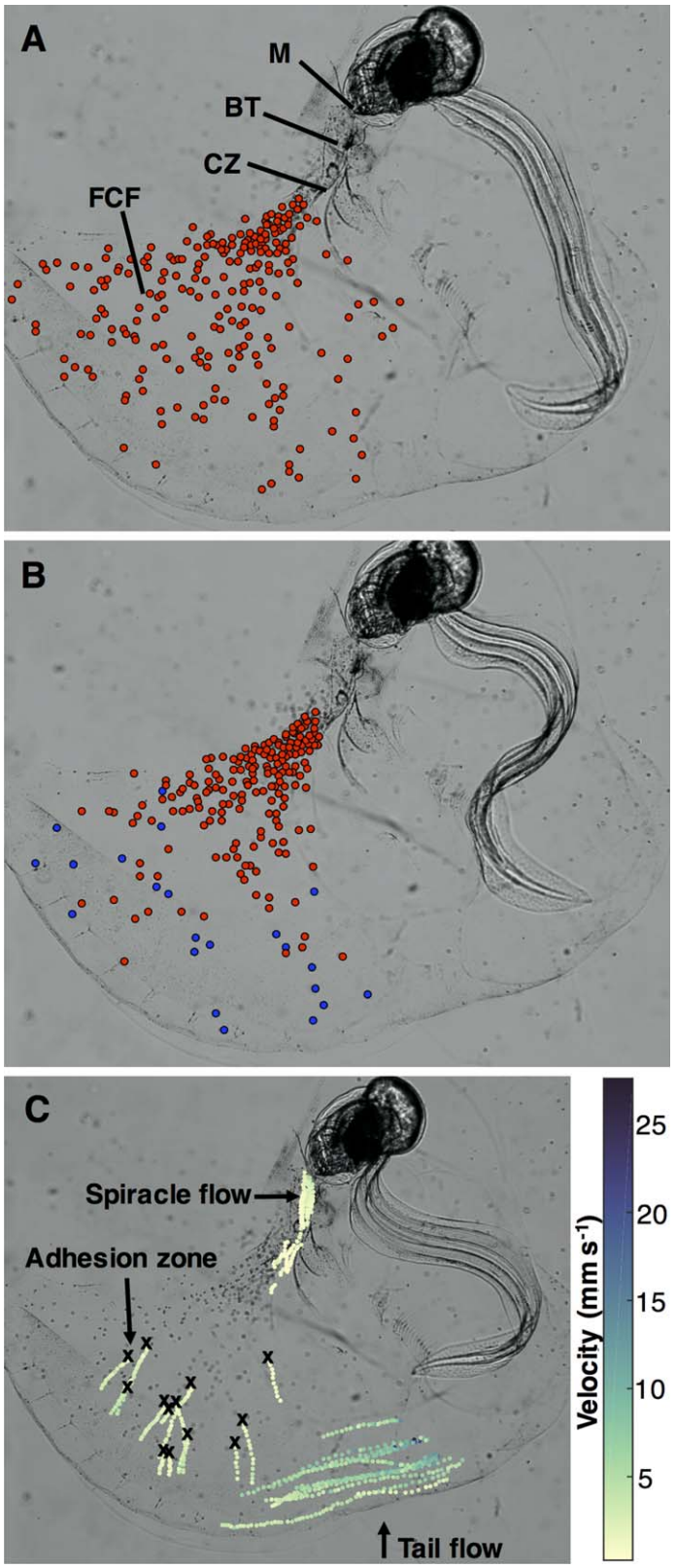

FCF, and the hypothesized role of filter elasticity, are summarized in Fig. 4.

Although Flood (1991) reported that the tail arrests serve to aggregate particles, we observed that beads remained mostly disaggregated (i.e., did not stick together) during conveyance through the FCF and buccal tube, and were usually captured as singlets by the pharyngeal filter. The deflation of the house during tail arrests reduced the inter-particle distance, but beads rarely adhered to each other when the FCF reinflated.

Particle adhesion to the FCF

Particle adhesion to the FCF following a tail arrest and reinflation cycle was consistently low (grand mean = 4.5% ± 5.6%, $n = 21$, $N = 7$) (Fig. 5). One outlying individual had 25% adhesion of 3 μm beads; however, this mean was calculated from comparatively few particles ($n = 1$ adhering particle out of four particles).

Particle size significantly affected adhesion (Kruskal-Wallis $\chi^2 = 8.344$, df = 2, $p = 0.0154$) (Fig. 5). Although no difference in adhesion was found between 3 μm and 6 μm beads ($p = 0.77$) or between 6 μm and 10 μm beads ($p = 0.117$), 3 μm beads adhered significantly more to the FCF than 10 μm beads ($p = 0.021$). Very few 20 μm beads of the mixed particle suspension were observed in the FCF, presumably because the width of the IF mesh, which is a function of the animal's body size, is of similar size (Lombard et al. 2010) and excluded these beads from entering the FCF.

Morphology and function of the intermediate screen

The milk bath allowed visualization of the coarse fibers of the intermediate layer of the FCF (Fig. 6). The fibers were arranged in a rectangular mesh with a mean width and length of $W = 22 \pm 7$ μm and $L = 160 \pm 22$ μm ($n = 25$, $N = 5$) (Fig. 6B). The length of the intermediate mesh was determined by the diameter of the filter ridges of the FCF. The margins of the ridges had vertical suspensory fibers connected to the lower and upper layers and crossed with the lateral fibers of the intermediate layers (Fig. 2B,E). The lateral fibers of the intermediate screen with deposited milk fat particles had a mean width of 2 ± 0.8 μm ($n = 25$, $N = 5$). Milk particles (< 1 μm) primarily collected on the lower layer (Fig. 6A), not the upper layer. Through milk-stained visualizations

Fig. 3. Impact of the tail on the distribution of *Rhinomonas* particles in the FCF of *O. dioica*. (**A**) Attached particles during the tail arrest cycle (red) and (**B**) pulse of detached particles collecting near the entrance of the buccal tube from the recommencement of the tail beating. Darker particles were not present in (**A**) but entered the filter from the tail chamber as the filters reinflated. (**C**) Map of adhesion of *Rhinomonas* particles to the FCF during continuous beating of the animal's tail. Black Xs show the location of particle adhesion. Heatmap shows particle velocities in the tail chamber, the FCF, and the buccal tube. BT, buccal tube; CZ, convergence zone; FCF, food-concentrating filter; M, mouth. [Color figure can be viewed at wileyonlinelibrary.com]

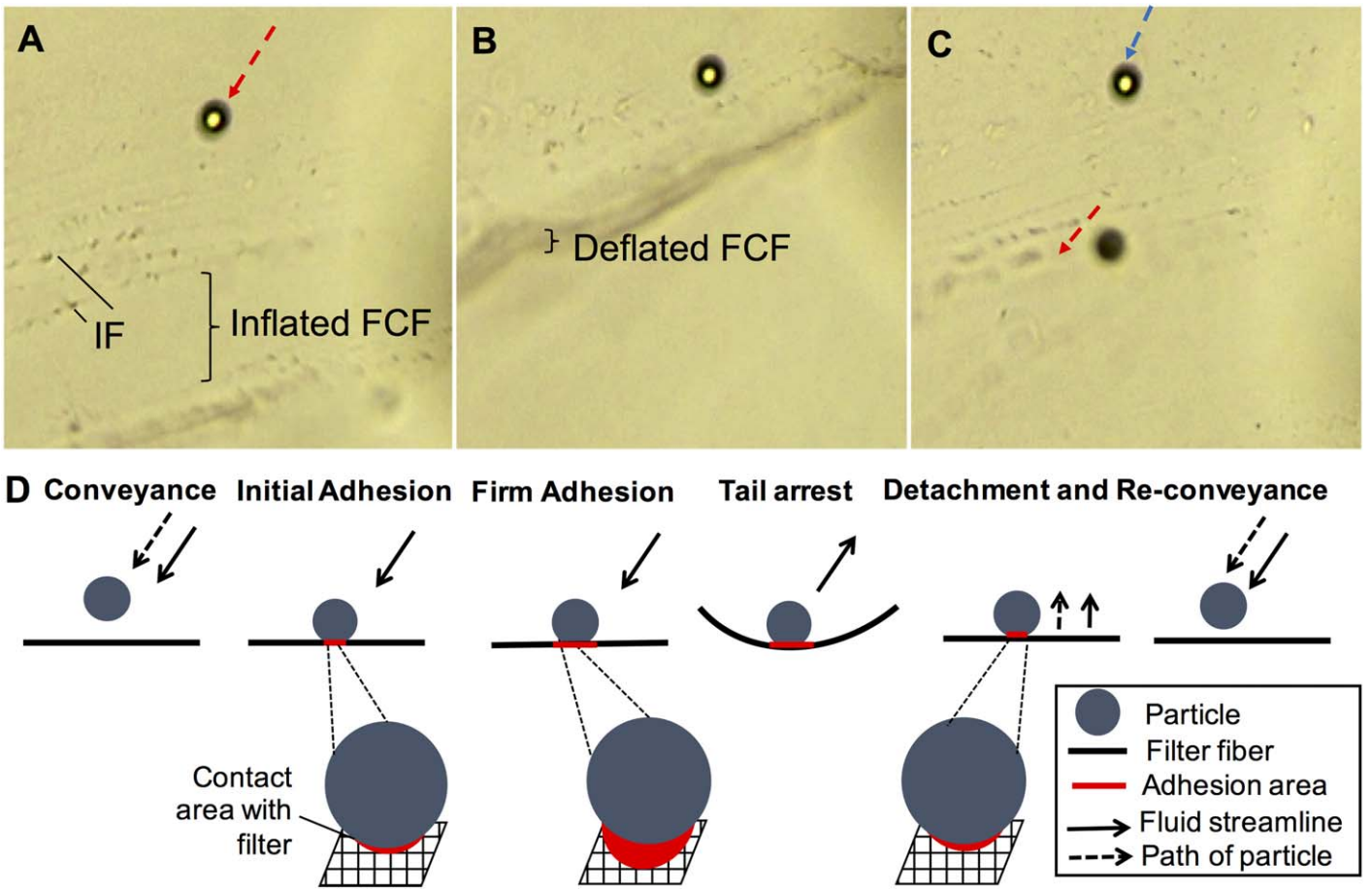

Fig. 4. The process of particle adhesion to and detachment from the FCF. (**A**) A 20 μm latex bead is conveyed laterally along the intermediate screen of the FCF (red arrow) toward the buccal tube due to the hydrostatic pressure generated by the animal's tail beating and by suction from the mouth. (**B**) Bead adheres to the FCF. A tail arrest deflates the FCF, which results in a temporary reversal of flow away from the buccal tube in a "backflush," and causes the individual mesh fibers of the intermediate screen to bend. (**C**) The tail resumes beating, the FCF reinflates and the mesh fibers return to their extended conformation, causing the bead to detach and move toward the buccal tube. Top arrow shows a new bead entering the field of view as a pulse of particles progresses down the FCF. (**D**) Schematic representation of the steps of the adhesion and detachment process that occur in (**A**–**C**), with the inferred changes in adhesive contact between the particle and the filter fiber. Firm adhesion occurs as time-dependent chemical adhesive interactions take place between the particle and the filter fiber. The elasticity of the fiber resets this process. [Color figure can be viewed at wileyonlinelibrary.com]

of the intermediate layer of the FCF, we were able to observe particles being conveyed directly along the intermediate screen (Fig. 6A).

Observations of feeding behavior

We observed that appendicularians are able to decouple filtration driven by tail beating from suction driven by the spiracles. Animals could draw particles into the house, but prevent the entry of particles from the FCF into the buccal tube through a previously undescribed mechanism. Flow could be halted at the convergence zone of the two fans of the FCF (Supporting Information Video 3) such that no particles entered the buccal tube while the buccal tube remained attached to the mouth. Alternatively, flow could enter the buccal tube and particle selection could be controlled through a valve in the buccal tube (Supporting Information Video 3). In the absence of suction from the mouth, the valve was forced open during the tail arrest, then resealed when tail beating resumed. When suction from the mouth caused flow into the buccal tube, the valve closed, sealed by the influx of water, even during tail arrests. Inverted flux from water forcefully exiting the mouth caused the valve to open and particles in the buccal tube were drawn into the exit chamber (Supporting Information Video 3).

At low frame rates, the ciliary spiracles appear to rotate due to a stroboscopic effect, but at higher frame rates the rotation is evidently a metachronal wave. The mechanism that accomplishes flow reversals to expel particles from the pharyngeal cavity has been vague, described as a "ciliary

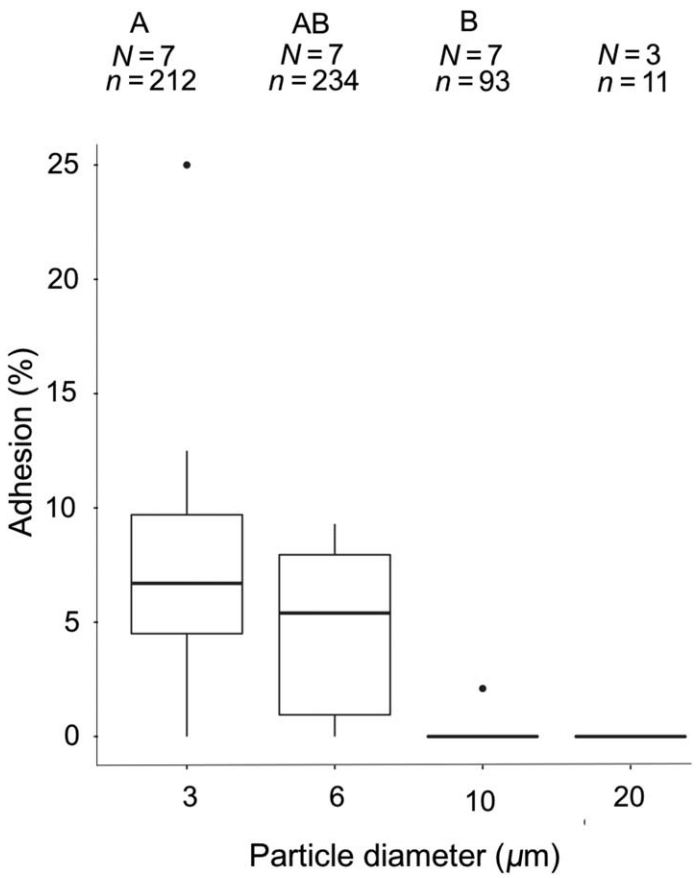

Fig. 5. Tukey box-and-whiskers plot showing the percentage adhesion of different sized latex microspheres to the FCF of *O. dioica*. Adhesion was calculated from the mean percent adhesion, summed across tail arrests for each animal. *N* indicates the number of animals from which mean percentage adhesion was measured, *n* indicates total number of particles analyzed from all animals. The letters A and B indicate significant differences with Nemenyi post hoc test.

reversal" that may involve a change in the orientation of cilia, a change in the direction of ciliary beating, or both (Galt and Mackie 1971; Fenaux 1986; Lombard et al. 2011). Although at lower frame rates (120 fps) this reversal appears to occur in the clockwise direction, this is due to stroboscopic effect. At high-speed (500 fps), we observed the reversal occurred only in the dorsal-ventral direction. Reversal of the ciliary beat direction changed the overall shape of the spiracles and appeared to reduce the size of the canal between the cilia (i.e., formed a constriction). Each episode of flow reversal was associated with such a constriction event (Supporting Information Video 4). Although the spiracles appear as a ring with uniform cilia (Supporting Information Video 4), transmission electron microscopy revealed that each of the spiracles contained two opposing clusters of cells with high densities of long cilia originating from each cluster (Fig. 7A). The spiracle cells were densely packed with mitochondria (Fig. 7B).

Discussion

We observed that the filtration process of *O. dioica* involved particles regularly attaching to and detaching from the FCF. The mechanism of the FCF is therefore not entirely analogous to an industrial tangential flow filtration system, where adhesion to the filter is generally low and usually irreversible (Altmann and Ripperger 1997). Rather, we describe the appendicularian FCF as a "self-cleaning filter" and provide a mechanistic explanation for how the FCF must detach particles in order for them to reach the pharyngeal filter for ingestion. Detachment only occurred after a tail arrest during reinflation of the filter, and most particle adhesion was reversed through this process (Fig. 5). We propose that detachment is caused by increased viscous drag on the particle as water flow increases through the FCF during

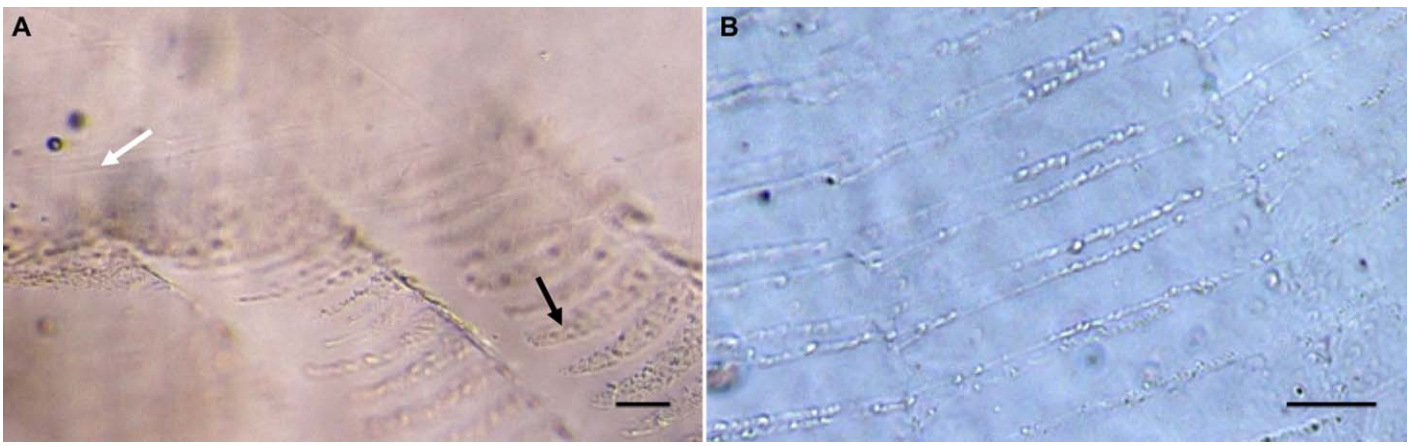

Fig. 6. Milk fat particles adhered to the FCF of *O. dioica*. (**A**) Black arrow shows colloidal milk particles caked on the lower layer of the FCF; white arrow shows the fibers of the intermediate screen suspended above the lower layer. A 10 μm microsphere is shown being conveyed along the intermediate screen. (**B**) The rectangular mesh of the intermediate screen of the FCF with adherent milk particles. Scale bars: 0.05 mm. [Color figure can be viewed at wileyonlinelibrary.com]

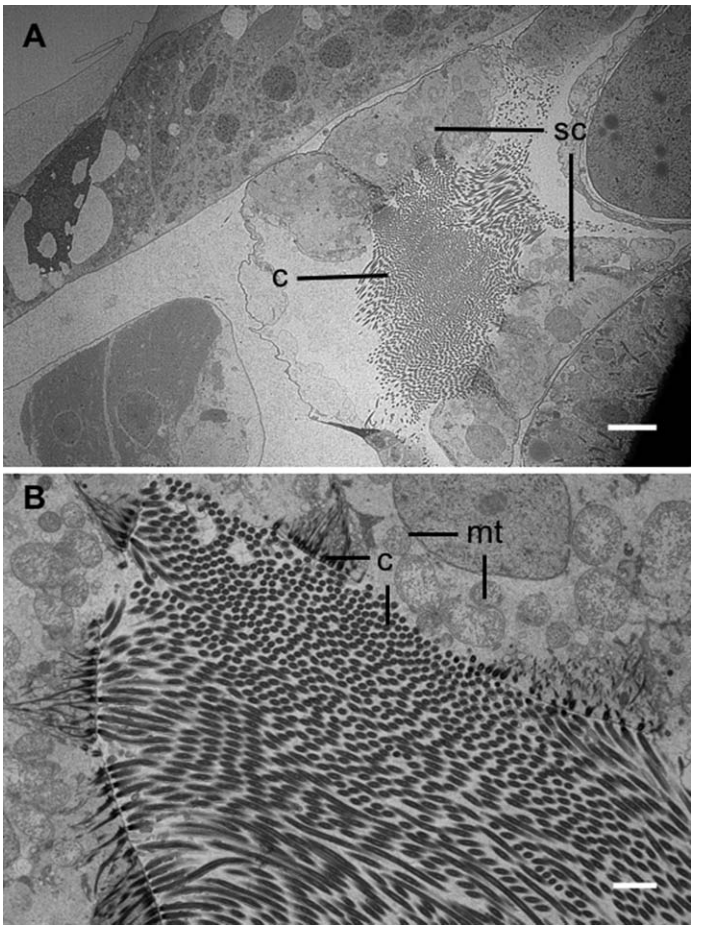

Fig. 7. Transmission electron micrographs of the ciliated spiracles of *O. dioica*. (**A**) Two clusters of spiracle cells (sc) showing densely packed cilia (c) (400X magnification). (**B**) Magnified view (1000X) of cilia showing the high density of mitochondria (mt). Scale bars: 10 μm in (**A**), 2 μm in (**B**).

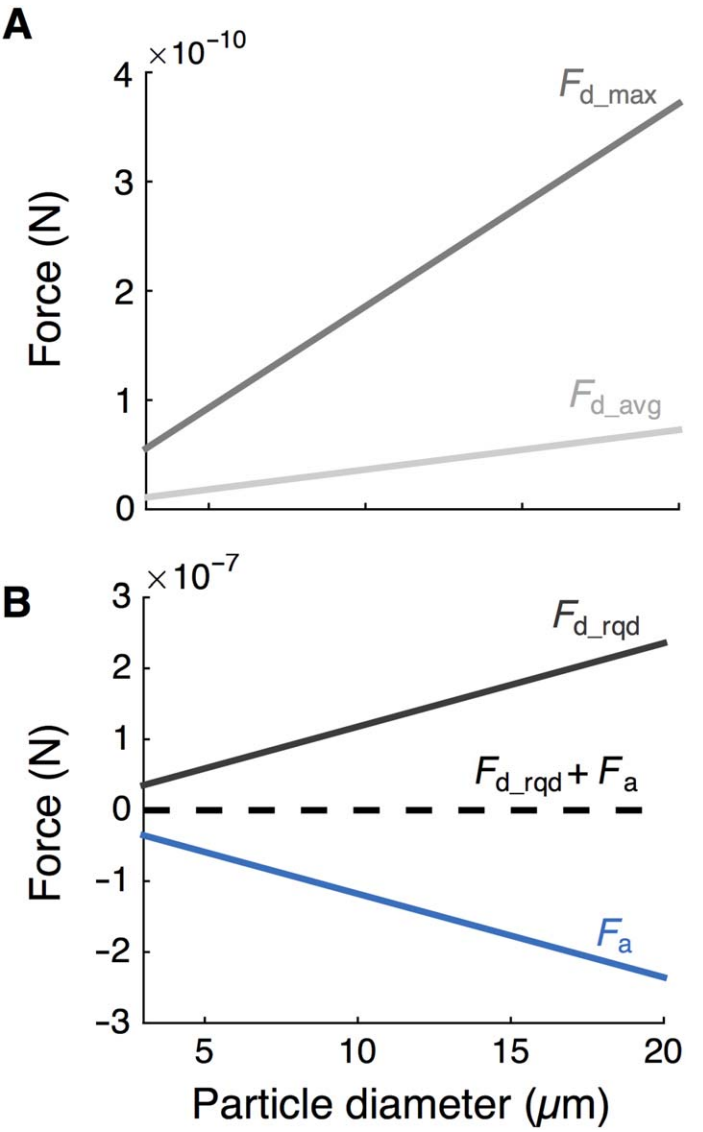

Fig. 8. Adhesion and detachment forces in the FCF. (**A**) Empirically calculated average and maximum Stokes drag force (F_d) on individual filter fibers of the FCF during filter reinflation after a tail arrest. (**B**) Theoretical Stokes drag force required ($F_{d\text{-}req}$) to equal the estimated attractive adhesion pull-off force (F_a). Dashed black line shows the sum of these forces. When $F_d - F_a < 0$, particles should remain adhered; when $F_d - F_a > 0$, particles should detach. [Color figure can be viewed at wileyonlinelibrary.com]

reinflation, combined with a reduction in contact area of the particle to the elastic mesh (Fig. 4, Supporting Information Video 1). We provide experimental evidence showing size-selective retention by the filter (Fig. 5), which is consistent with the size-dependent detachment patterns predicted by Stokes drag force (Fig. 8A). Collectively, these results provide a mechanistic basis for understanding particle selection by these ecologically important grazers.

Theoretical framework of adhesion and detachment forces

Pulsatile flow generated by the tail arrest has previously been acknowledged to play an important role in clearing the IF of accumulated particles (Flood 2003; Selander and Tiselius 2003; Tiselius et al. 2003), but its role in particle progression along the FCF has heretofore been less widely recognized (Flood 1978). To test if pulsatile flow alone can explain the detachment process, we can simplify the system of the FCF to two forces: the drag force for detachment (F_d) and the adhesion force (F_a). Because particle collection by appendicularians occurs in laminar flow at low Reynolds numbers (Morris and Deibel 1993; Acuña, Deibel, and Morris 1996), we can use a modified Stokes drag, which increases linearly with particle size as:

$$F_d = 1.7009 \cdot 6\pi\mu r v$$

where μ is the dynamic viscosity of seawater (1.07×10^{-3} kg m^{-1} s^{-1}), r is the radius of the sphere (1.5×10^{-6}–1×10^{-5} μm),

v is the velocity (m s^{-1}), and 1.7009 is a constant to account for the effect of a surface near the fluid stream (O'Neill 1968; Burdick et al. 2001). F_d is calculated from the average (1.9×10^{-4} m s^{-1}) and maximum (9.7×10^{-4} m s^{-1}) instantaneous velocities of the intermediate filter fibers during a reinflation of the house to estimate the respective changes in the drag force caused by pulsatile flow (Fig. 8A). Although the adhesive interactions between particles and the mucus filter are complex and beyond the scope of the present study, we estimate the adhesive force using the Johnson, Kendall, and Roberts (JKR) model of adhesive elastic contacts, where the pull-off force required to detach an elastic sphere from a hard, flat substrate scales linearly with the particle radius as:

$$F_a = -\frac{3}{2}\pi\omega R$$

where ω is the surface energy (J m^{-2}) due to the van der Waals interactions between the particle and the substrate (Johnson et al. 1971; Persson 2003) and R is the radius of curvature, here assumed equivalent to $\frac{1}{2}r$ (Attard and Parker 1992). Although the surface energy is unknown, 0.01 J m^{-2} represents a conservatively low, biologically relevant estimate (Gay 2002). Pulsatile flow caused by the tail arrest and reinflation cycle increased the Stokes drag force by an order of magnitude when calculated from the average and maximum fiber velocities (Fig. 8A). However, these empirically calculated values of F_d (Fig. 8A) were both orders of magnitude lower than the estimates of F_a (Fig. 8B). Our results, therefore, support our first hypothesis that pulsed flow facilitates particle detachment, but pulsed flow may not be the sole mechanism for detachment since our calculations of increased viscous drag alone cannot account for our observations that particle detachment consistently occurs after a reinflation of the house.

Numerous factors may account for the inadequate drag force compared to the estimated adhesive force. One possible explanation for the discrepancy is that the conformational changes of the fibers occur at instantaneous velocities rapid enough to impose sufficient drag. We used the change in arc length to measure the overall conformational change of the fibers from relaxed to straight, which occurs over multiple tail beats during reinflation of the FCF ($\sim$ 0.5 s, 250 frames on our camera). However, the fibers stiffen abruptly (often in less than 2 ms, or 1 frame) over very short distances (a few microns), and these spatial and temporal resolution limitations affect the maximum velocity that we can measure (Adrian 1991) during the period of fiber stiffening. Thus, our measured maximum instantaneous velocity of the fibers (Supporting Information Video 1) is likely an underestimate. In order to mathematically satisfy the fiber velocity that would be required to overcome the adhesion force (i.e., for $v > \frac{F_a}{1.7009 \cdot 6\pi\mu r}$), an instantaneous velocity of $\sim$ 0.6 m s^{-1}, or a drag force of 10^{-7}–10^{-8} N, would be required (Fig. 8B) and an intermediate Reynolds number of 1. Although this speed may seem prohibitively fast, there are numerous biological examples of small, cellulose-based structures that passively achieve speeds up to an order of magnitude greater than this (Edwards et al. 2005; Nimmo et al. 2014; Forterre et al. 2016), and therefore could provide a mechanistic explanation for particle detachment by the appendicularian FCF. However, further investigation of the adhesive forces involved and the precise detachment mechanism is required.

Experimental observations of adhesion and detachment

The elasticity of the filter may also facilitate particle detachment in other ways. Deformable materials can undergo time-dependent adhesion, whereby the contact area between the particle and the substrate increases the longer the two are in contact (Krishnan et al. 1994) (Fig. 4D). Thus, as appendicularians filter-feed and accumulate adhered particles on the FCF, it should seemingly become more difficult to detach particles the longer the particles remain adhered. We propose that the pulsatile flow caused by periodic tail arrests and the associated elastic behavior of the filter fibers act in concert to counteract this problem: the elastic recoil of the filter following a tail arrest and filter reinflation cycle reduces the contact area between the particle and the filter fiber, reducing the adhesive force and facilitating detachment (Fig. 4D). The importance of fiber elasticity as a driving mechanism for detachment is supported by our observation that particle detachment occurred most frequently on the outer margins of the FCF (Fig. 3A,B; Supporting Information Video 2). Because the distance between the lateral fibers and suspensory fibers shortens toward the buccal tube (Fig. 2D), the lateral fibers at the outer margins of the FCF are able to deform more during deflation than lateral fibers closer to the buccal tube. This increased deformation produces greater adhesive area change that favors detachment at the filter margins. The elasticity of the filter may also indirectly aid detachment by increasing the achievable peak flow rate and increasing shear stress at the walls (San and Staples 2012).

Historically, appendicularians have been assumed to feed non-selectively (Bedo et al. 1993; Acuña et al. 1996; Gorsky et al. 1999). Our results, however, show that size-dependent adhesion may cause selective particle retention by the appendicularian house, with smaller particles being more likely to remain adhered to the FCF (Fig. 5). We therefore reject our second hypothesis that no size-selection by the house occurs through particle interactions with the FCF. This study is the first to isolate particle retention by the FCF, and therefore, it is difficult to make direct comparisons with prior results on size-retention by the whole house, since particles may exhibit different adhesion patterns onto different house components (house walls, IF, or FCF). For example, the combined animal (*O. dioica*) and house system retained smaller beads with lower efficiency (Fernández et al. 2004), but, since these measurements were influenced by the pharyngeal filter, this finding does not conflict with our results. Fernández et al. (2004) also showed reduced retention of the largest beads (6 μm) by the IF of small animals. Similarly, Conley and Sutherland (In press) showed 10 μm beads were

positively selected in the houses of *O. dioica* compared to 3 μm ones; however, it is likely that 10 μm beads mostly adhered to the IF rather than the FCF. They found smaller particles (0.3 μm) were consistently higher in the house than larger ones (1.75 μm), which supports our observations of size-selection by the FCF. Previous flow cytometric analysis of *O. dioica* houses showed 0.2 μm beads accumulated in the house at a higher rate than 0.75 μm ones (Bedo et al. 1993). Although Bedo et al. (1993) proposed that the 0.2 μm beads adhered to the internal house walls, it is probable that adhesion to the FCF also contributed. Smaller particles are also known to accumulate more on the membranes of industrial crossflow filtration systems (Stamatakis and Tien 1993). Collectively, these observations suggest that appendicularian houses may exhibit a bimodal distribution of accumulated particles: large particles adhered to the IF and small particles adhered to the FCF.

In general, however, we found that adhesion across particle sizes was consistently low for a single tail arrest and reinflation cycle—attesting to the efficacy of the self-cleaning ability of the FCF. Bochdansky and Deibel (1999) offered wide bounds for the loss of particles in the appendicularian house ($\sim$ 15–300%), but only one prior measurement has been made for the adhesion to the house: an estimated $\sim$ 30% of filtered phytoplankton ($<$ 30 μm) removed by *O. dioca* remained adhered over the lifetime of the house (Gorsky et al. 1984). Since this estimate included particle adhesion to the entire house, it provides an upper bound for the overall percentage adhesion of particles to the FCF over multiple tail arrests. Undoubtedly, particle sizes, types, and concentrations also influence overall adhesion to the house, and as the house ages and the IF become clogged, pulsatile flow may become less effective at detaching particles. Nevertheless, our results show that, under our experimental conditions, the FCF is quite effective at detaching adhered particles through a single tail arrest and reinflation cycle. The frequent replacement of the entire house by newly synthesized and inflated structures (approximately every 4 h for *O. dioica* at 15°C, Troedsson et al. 2009) also provides a regular filter system reset to overcome accumulated adhesive clogging.

Function of the intermediate screen

The functional role of the intermediate layer of the appendicularian FCF has remained uncertain, with speculation that it serves a purely structural role (Deibel 1986), or possibly a straining function (Alldredge 1977). Although the intermediate layer certainly serves a structural role in connecting the upper and lower layers of the FCF as previously suggested (Deibel 1986), it is evident that various sizes of particles, from 20 μm beads (Fig. 4A–C) to milk fat and charcoal particles (Fig. 6, Deibel 1986), interact directly with the intermediate screen and sometimes adhere to its fibers. The intermediate fibers, like the rest of the FCF, exhibited a marked deformability (Fig. 2E,F). Therefore, we reject our third hypothesis that the intermediate layer serves a solely structural role, since our results show it is involved in particle collection and that the elasticity of its fibers may facilitate particle detachment.

Observations of feeding behavior

Our observations of the valve in the buccal tube (Supporting Information Video 3) and the role of the spiracles in flow reversals help further explain appendicularian feeding behavior. Fenaux (1986) described two valve-like openings on either side of buccal tube through which filtered water exits the buccal tube; however, we observed only one valve in the center of the tube (Supporting Information Video 3). We believe the center valve is the same structure previously described as two side valves, since the stream of ejected particles makes it appear that the valve is located on the side (Supporting Information Video 3). Lombard et al. (2011) described a "pipe-smoking" behavior in which reversal of the ciliary beat of the spiracles causes particle rejection into the exit chamber. Our findings suggest that the valve in the buccal tube provides an additional pathway for pipe-smoking behavior.

Furthermore, our observations lessen some ambiguity regarding the mechanism of the previously described "ciliary reversals" (Galt and Mackie 1971). Our video observations show that, during a reversal, the ciliary beat does not reverse in the clockwise direction, but does reorient in the dorsal-ventral direction. This reorientation appears to reduce the effective diameter of the spiracle funnel, forming a constriction that is associated with flow reversal (Supporting Information Video 4). The ultrastructure of the spiracles has been previously described for *Kowalevskia tenuis*, *Kowalevskia oceanica* (Brena et al. 2003), and *O. dioica*. (Burighel et al. 2001). Our transmission electron micrographs show the spiracle structure of *O. dioica* at higher magnification than previous observations from thick sections (Burighel et al. 2001), revealing the fine structure of the two tufts of cilia that compose each spiracle. The density of mitochondria suggests a very high-energy demand for the spiracles. Collectively, these observations yield insights into the form and function of the spiracles—namely, how they move, drive flow into the pharynx, and facilitate particle rejection.

Implications

While particle-filter adhesion is a micro-scale process, understanding the effect of adhesion on selective particle retention by marine grazers has predictive value for large-scale processes such as carbon transformation and transport. The implications of particle adhesion to the appendicularian FCF is of particular importance because appendicularians represent a shortcut in the aquatic trophic web, linking ultraplankton directly to many marine fish (Purcell et al. 2005). Particles that adhere to the appendicularian house are more nutritive than those packaged in the refractory fecal pellets (Bochdansky and Deibel 1999). Because of this, discarded houses are preyed upon by numerous taxa, including calanoid and harpacticoid copepods, euphausiid larvae, and

flat, forage, and reef fishes, and contribute to remineralization of particulate organic carbon in the ocean (Alldredge 1976; Steinberg et al. 1994; Purcell et al. 2005).

References

Acuña, L. J., D. Deibel, and C. C. Morris. 1996. Particle capture mechanism of the pelagic tunicate *Oikopleura vanhoeffeni*. Limnol. Oceanogr. **41**: 1800–1814. doi:10.4319/lo.1996.41.8.1800

Adrian, R. J. 1991. Particle-imaging techniques for experimental fluid mechanics. Annu. Rev. Fluid Mech. **23**: 261–304. doi:10.1146/annurev.fl.23.010191.001401

Alldredge, A. L. 1976. Discarded appendicularian houses as sources of food, surface habitats, and particulate organic matter in planktonic environments. Limnol. Oceanogr. **21**: 14–23. doi:10.4319/lo.1976.21.1.0014

Alldredge, A. L. 1977. House morphology and mechanisms of feeding in the Oikopleuridae (Tunicata, Appendicularia). J. Zool. **181**: 175–188. doi:10.1111/j.1469-7998.1977.tb03236.x

Altmann, J., and S. Ripperger. 1997. Particle deposition and layer formation at the crossflow microfiltration. J. Memb. Sci. **124**: 119–128. doi:10.1016/S0376-7388(96)00235-9

Attard, P., and J. L. Parker. 1992. Deformation and adhesion of elastic bodies in contact. Phys. Rev. A **46**: 7959. doi:10.1103/PhysRevA.46.7959

Bedo, A. W., J. L. Acuña, D. Robins, and R. P. Harris. 1993. Grazing in the micron and the sub-micron particle size range: The case of *Oikopleura dioica* (Appendicularia). Bull. Mar. Sci. **53**: 2–14.

Bochdansky, A. B., and D. Deibel. 1999. Measurement of in situ clearance rates of *Oikopleura vanhoeffeni* (Appendicularia: Tunicata) from tail beat frequency, time spent feeding and individual body size. Mar. Biol. **133**: 37–44. doi:10.1007/s002270050440

Bouquet, J. M., E. Spriet, C. Troedsson, H. Otterå, D. Chourrout, and E. M. Thompson. 2009. Culture optimization for the emergent zooplanktonic model organism *Oikopleura dioica*. J. Plankton Res. **31**: 359–370. doi:10.1093/plankt/fbn132

Brainerd, E. L. 2001. Caught in the crossflow. Nature **412**: 387–388. doi:10.1038/35086666

Brena, C., F. Cima, and P. Burighel. 2003. Alimentary tract of Kowalevskiidae (Appendicularia, Tunicata) and evolutionary implications. J. Morphol. **258**: 225–238. doi:10.1002/jmor.10145

Burdick, G. M., N. S. Berman, and S. P. Beaudoin. 2001. Describing hydrodynamic particle removal from surfaces using the particle Reynolds number. J. Nanopart. Res. **3**: 453–465. doi:10.1023/A:1012593318108

Burighel, P., C. Brena, G. B. Martinucci, and F. Cima. 2001. Gut ultrastructure of the appendicularian *Oikopleura dioica* (Tunicata). Invertebr. Biol. **120**: 278–293. doi:10.1111/j.1744-7410.2001.tb00038.x

Conley, K. R., and K. R. Sutherland. 2017. Particle shape controls export and fate in the ocean through interactions with the globally abundant grazer *Oikopleura dioica*. PLOS ONE **12**: e0183105. doi:10.1371/journal.pone.0183105

Deibel, D. 1986. Feeding mechanism and house of the appendicularian *Oikopleura vanhoeffeni*. Mar. Biol. **93**: 429–436. doi:10.1007/BF00401110

Deibel, D. 1988. Filter feeding by *Oikopleura vanhoeffeni*: Grazing impact on suspended particles in cold ocean waters. Mar. Biol. **99**: 177–186. doi:10.1007/BF00391979

Edwards, J., D. Whitaker, S. Klionsky, and M. J. Laskowski. 2005. Botany: A record-breaking pollen catapult. Nature **435**: 164–164. doi:10.1038/435164a

Fenaux, R. 1986. The house of *Oikopleura dioica* (Tunicata, Appendicularia): Structure and functions. Zoomorphology **106**: 224–231. doi:10.1007/BF00312043

Fernández, D., A. López-Urrutia, A. Fernández, J. L. Acuña, and G. Harris. 2004. Retention efficiency of 0.2 to 6 μm particles by the appendicularians *Oikopleura dioica* and *Fritillaria borealis*. Mar. Ecol. Prog. Ser. **266**: 89–101. doi:10.3354/meps266089

Flood, P. R. 1978. Filter characteristics of appendicularian food catching nets. Experientia **34**: 173–175. doi:10.1007/BF01944659

Flood, P. R. 1991. Architecture of, and water circulation and flow rate in, the house of the planktonic tunicate *Oikopleura labradoriensis*. Mar. Biol. **111**: 95–111. doi:10.1007/BF01986351

Flood, P. R. 2003. House formation and feeding behaviour of *Fritillaria borealis* (Appendicularia: Tunicata). Mar. Biol. **143**: 467–475. doi:10.1007/s00227-003-1075-y

Flood, P. R., and D. Deibel. 1998. The appendicularian house. *In* Q. Bone [ed.], The biology of pelagic tunicates. Oxford Univ. Press. p. 105–124.

Forterre, Y., P. Marmottant, C. Quilliet, and X. Noblin. 2016. Physics of rapid movements in plants. Europhys. News **47**: 27–30. doi:10.1051/epn/2016104

Galt, C. P., and G. O. Mackie. 1971. Electrical correlates of ciliary reversal in *Oikopleura*. J. Exp. Biol. **55**: 205–212.

Gay, C. 2002. Stickiness—some fundamentals of adhesion. Integr. Comp. Biol. **42**: 1123–1126. doi:10.1093/icb/42.6.1123

Gemmell, B. J., H. Jiang, and E. J. Buskey. 2014. A new approach to micro-scale particle image velocimetry (μPIV) for quantifying flows around free-swimming zooplankton. J. Plankton Res. **36**: 1396–1401. doi:10.1093/plankt/fbu067

Gorsky, G., N. S. Fisher, and S. W. Fowler. 1984. Biogenic debris from the pelagic tunicate, *Oikopleura dioica*, and its role in the vertical transport of a transuranium element. Estuar. Coast. Shelf Sci. **18**: 13–23. doi:10.1016/0272-7714(84)90003-9

Gorsky, G., and R. Fenaux. 1998. The role of Appendicularia in marine food webs. *In* Q. Bone [ed.], The biology of pelagic tunicates. Oxford Univ. Press. p. 161–169.

Gorsky, G., M. J. Chrétiennot-Dinet, J. Blanchot, and I. Palazzoli. 1999. Picoplankton and nanoplankton aggregation by appendicularians: Fecal pellet contents of *Megalocercus huxleyi* in the equatorial Pacific. J. Geophys. Res. C Oceans **104**: 3381–3390. doi:10.1029/98JC01850

Johnson, K. L., K. Kendall, and A. D. Roberts. 1971. Surface energy and the contact of elastic solids. Proc. R. Soc. Lond. A **324**: 301–313. doi:10.1098/rspa.1971.0141

Katija, K., R. E. Sherlock, A. D. Sherman, and B. H. Robison. 2017. New technology reveals the role of giant larvaceans in oceanic carbon cycling. Sci. Adv. **3**: e1602374. doi: 10.1126/sciadv.1602374

Krishnan, S., A. A. Busnaina, D. S. Rimai, and L. P. Demejo. 1994. The adhesion-induced deformation and the removal of submicrometer particles. J. Adhes. Sci. Tech. **8**: 1357–1370. doi:10.1163/156856194X00654

Liu, K., and L. Jiang. 2012. Bio-inspired self-cleaning surfaces. Annu. Rev. Mat. Res. **42**: 231–263. doi:10.1146/annurev-matsci-070511-155046

Lombard, F., D. Eloire, A. Gobet, L. Stemmann, J. R. Dolan, A. Sciandra, and G. Gorsky. 2010. Experimental and modeling evidence of appendicularian-ciliate interactions. Limnol. Oceanogr. **55**: 77–90. doi:10.4319/lo.2010.55.1.0077

Lombard, F., E. Selander, and T. Kiørboe. 2011. Active prey rejection in the filter-feeding appendicularian *Oikopleura dioica*. Limnol. Oceanogr. **56**: 1504–1512. doi:10.4319/lo.2011.56.4.1504

Meijering, E., O. Dzyubachyk, and I. Smal. 2012. Methods for cell and particle tracking. Methods Enzymol. **504**: 183–200. doi:10.1016/B978-0-12-391857-4.00009-4

Morris, C. C., and D. Deibel. 1993. Flow rate and particle concentration within the house of the pelagic tunicate *Oikopleura vanhoeffeni*. Mar. Biol. **115**: 445–452. doi:10.1007/BF00349843

Nimmo, J. R., P. M. Hermann, M. B. Kirkham, and E. R. Landa. 2014. Pollen dispersal by catapult: Experiments of Lyman J. Briggs on the flower of Mountain Laurel. Phys. Perspect. **16**: 371–389. doi:10.1007/s00016-014-0141-9

O'Neill, M. 1968. A sphere in contact with a plane wall in a slow linear shear flow. Chem. Eng. Sci. **23**: 1293. doi: 10.1016/0009-2509(68)89039-6

Persson, B. N. J. 2003. On the mechanism of adhesion in biological systems. J. Chem. Phys. **118**: 7614–7621. doi: 10.1063/1.1562192

Purcell, J. E., M. V. Sturdevant, C. P. Galt, M. J. Youngbluth, and D. Deibel. 2005. A review of appendicularians as prey of invertebrate and fish predators, p. 359–435. *In* G. Gorsky, M. J. Youngbluth, and D. Deibel [eds.], Response of marine ecosystems to global changes: Ecological impact of appendicularians. GB Scientific.

Riisgård, H. U., and P. S. Larsen. 2001. Minireview: Ciliary filter feeding and bio-fluid mechanics—present understanding and unsolved problems. Limnol. Oceanogr. **46**: 882–891. doi:10.4319/lo.2001.46.4.0882

Rubenstein, D. I., and M. A. R. Koehl. 1977. The mechanisms of filter feeding: Some theoretical considerations. Am. Nat. **111**: 981–994. doi:10.1086/283227

San, O., and A. E. Staples. 2012. Dynamics of pulsatile flows through elastic microtubes. Int. J. App. Mech. **4**: 1250006. doi:10.1142/S175882511200135X

Selander, E., and P. Tiselius. 2003. Effects of food concentration on the behaviour of *Oikopleura dioica*. Mar. Biol. **142**: 263–270. doi:10.1007/s00227-002-0949-8

Sommer, U., and H. Stibor. 2002. Copepoda–Cladocera–Tunicata: The role of three major mesozooplankton groups in pelagic food webs. Ecol. Res. **17**: 161–174. doi:10.1046/j.1440-1703.2002.00476.x

Stamatakis, K., and C. Tien. 1993. A simple model of cross-flow filtration based on particle adhesion. AIChE J. **39**: 1292–1302. doi:10.1002/aic.690390805

Steinberg, D. K., M. W. Silver, C. H. Pilskaln, S. L. Coale, and J. B. Paduan. 1994. Midwater zooplankton communities on pelagic detritus (giant larvacean houses) in Monterey Bay, California. Limnol. Oceanogr. **39**: 1606–1620. doi: 10.4319/lo.1994.39.7.1606

Thompson, E. M., T. Kallesøe, and F. Spada. 2001. Diverse genes expressed in distinct regions of the trunk epithelium define a monolayer cellular template for construction of the oikopleurid house. Dev. Biol. **238**: 260–273. doi:10.1006/dbio.2001.0414

Tiselius, P., and others. 2003. Functional response of *Oikopleura dioica* to house clogging due to exposure to algae of different sizes. Mar. Biol. **142**: 253–261. doi:10.1007/s00227-002-0961-z

Troedsson, C., J. M. Bouquet, R. Skinnes, J. Acuna, K. Zech, J. E. Frischer, and E. M. Thompson. 2009. Regulation of filter-feeding house components in response to varying food regimes in the appendicularian, *Oikopleura dioica*. J. Plankton Res. **31**: 1453–1463. doi:10.1093/plankt/fbp085

Acknowledgments

We thank three anonymous peer reviewers, whose feedback greatly improved the manuscript. We thank the staff of the appendicularian culture facility at Sars for providing animals for the study and Raghu Parthasarathy for valuable discussions on the physics of elastic deformation. This work was supported in part by grants from the National Science Foundation OCE-1537201 (to K. R. S.), CBET-1511996 (to B. J. G.), OCE-1537546 (to B. J. G.), and the Norwegian Research Council, NFR-HK 204040/E40 and NFR 133335/V40 (to E. M. T.). K. R. C. was supported in part by an Oregon Sea Grant 2014 Robert E. Malouf Marine Studies Scholarship.

Conflict of Interest

None declared.

Submitted 22 October 2016
Revised 01 March 2017; 07 July 2017; 09 August 2017
Accepted 14 August 2017

Associate editor: Thomas Kiørboe